EXPERIMENTAL AND FINITE ELEMENT ANALYSIS OF NONAXISYMMETRIC STRETCH FLANGING PROCESS USING AA 5052

DOI : 10.36909/jer.ICIPPSD.15501

Sachin Kumar Nikam*, Sandeep Jaiswal

Department of Engineering and Technology, LNCT University, Bhopal, Madhya Pradesh 462042, India.

*Email: sacinkumarnikam@gmail.com; Corresponding Author.

ABSTRACT

This paper deals with experimental and finite element analysis of the stretch flanging process using AA- 5052 sheets of 0.5 mm thick. A parametrical study has been done through finite element simulation to inspect the influence of procedural parametrical properties on maximum thinning (%) within the stretch flanging process. The influence of preliminary flange length of sheet metal blank, punch die clearance, and width was examined on the maximum thinning (%). An explicit dynamic finite element method was utilized using the finite element commercial package ABAQUS. Strain measurement was done after conducting stretch flanging tests. A Mesh convergence examination was carried out to ascertain the maximum percentage accuracy in FEM model. It is found through finite element simulation that the width of sheet metal blanks has a greater impact on the maximum percentage of thinning as compared to preliminary flange length, and clearance of the punch dies.

Key words: Flanging, finite element method, preliminary length of flange, simulation, clearance of punching die, width, thinning.

INTRODUCTION

As we know in sheet metal forming process flanging known as shape deforming process which is widely used in the auto manufacturing sector. Flanging basically a deforming operational procedural in which sheet metal can be deform usually to 90^0 degrees to improve edge strength of sheet metal parts with finished rounded edge along with highest value of rigidity. In the auto manufacturing sector, some part which having critical joint which is not disappear normally can also produce by this operation. There are various types of flanging processes as shown in Fig.1 (Asnafi, 1999). Classification according to deformation flanging can be 2 types one is shrinkable and the other one is stretchable as seen in fig.2 (Asnafi, 1999).

In shrinkable flanging process the curve profile of flange is convex and metal undergoes compression in the peripheral direction. In this operation, the length of arc of the finished flange is least as compared to initial arc length of the element. In this process, at top level of flange compression value is high and minimum at radial profile of die. In other end if the curve profile of the flange is concave and sheet metal undergoes in tension at peripheral direction this process is known as the stretchable flanging process. The value of tension is high at top level of the flange and length of arc also increases. Various studies have already been carried out in this field of flanging process to identified result-oriented evidence-based examination on the effect of various formability parameters of flanging using FEM-based model analysis, experimentally evidence, and theoretical based approach. In past, some researchers studied the problems of flanging using total plasticity theories (Wang et al., 1974, Wang, 1983). However, there was less work was reported on the theoretical research for the problems involved in flanges, such as for the prediction method of flanging height, especially in the case of shrink flanging. Besides this, analytical models were also presented to examine the deportment of shrink and stretch flanges (Wang and Wenner, 1974); Wang et al., 1974). Both models were effectively used for the analysis of the flanging process, but it was difficult due to complex mathematical formulae to be applied by designers who want to predefine the blank shape. Also, both models were not able to consider the effect on the planar anisotropy of the flanging process. In this regard, analytical models were also proposed for introversion/stretch and outcurve/ hrink flange which considered into an account of the effect of planar anisotropy for flanging process as well as unifies both above models for prediction of blank's trim line and shape of a rolling –stock's retractor (Hu et al,2003).

In a view of trimline development and formability of stretch flanges models for an axisymmetric case and finite element simulation method for the non-axisymmetric case were developed for estimation of trimline and extreme level of strain (Dudraand Shah, 1988). The axisymmetric model can be used for the prediction of peak strain for most flange geometries while the FEM model may be used to develop trimline for stretch flanges. In addition to this, in the case of prediction of trimming line for curved flanging an efficient procedure was obtained by connecting with One-step analysis (Bao and Huh, 2007). The 1-step analysis was found to be more accurate than the conventional section method and can be applied during the design of die for edging as an important process. The 1-step analysis was found to be more accurate than the conventional section method and can be applied during the design of

die for edging as an important process.

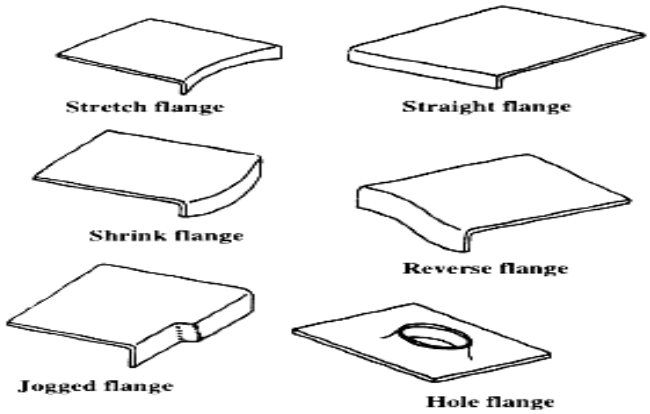

Figure 1 Different type of flanges (Asnafi N., 1999).

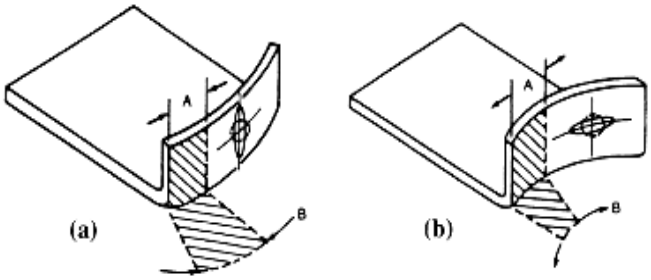

Figure 2 Sheet metal process (a) shrinkage flanging (b) stretchable flanging (Asnafi N., 1999).

In stretchable flanging of Vee-shaped blanks, a similar 2D FEM and an elastic FEM and plastic FEM program respectively were used to analyze the influence of different material and its parametrical characteristics on the deformability of flange (Wang et al. (1984), Li et al, 2007). In another case of the stretch flanging process, the forward -inverse prediction model was used to optimize blank shape with the integration of explicit dynamic FEM, absolute strain methodology, or fuzzy inference system depend on adaptive network (Yeh et al., 2007). During stretchable flanging, the governing condition of failing along the edge side is depends on two factor one is fracture another is local necking. In the stretch flanging of AKDQ steel, a local necking failure was suggested which is depend on the criterion of hill's instability considered the effect of plastic anisotropy and strain to harden (Wang et al., 1995). When the plastic strain ratio of aluminum alloys increased using stretch flanging by fluid forming highest fracture limit was obtained it also depends on plastic strain ratio increment and exponent of strain hardening (Asnafi, 1999). If we used simulation technique which is

based on numeric calculation for stretchable flange operation to predict strain within the stretch, we got flange features that having more accuracy with Barlat-89 and Hill-48 yield criteria as compared to von Mises yield criteria (Worswick and Finn,2000). To avoid fracture at the fringe of the flange in the stretchable deformation process we have to keep flange height small and also maintain a least ratio of straight side length to the curvature radial range were recommended in stretchable curve flanging (Feng X. et al., 2004). Wrinkles were obtained into the outer part of stretched z-flanging deformation with draw-bead which can be controlled by adjustment of blank holding force (Vafaeesefat and Khanahmadlee M., 2011). In FEM simulation of stretching flange process the idea of continuum mechanics turned into hired by numerous research specialists for the prophecy of failure. A multi-scale FEM destruction model executed for simulation of stretchable flanging process of Aluminum Alloy of 5182 and Aluminum Alloy 5754(Chen et al, 2005). similarly, to this, lower band destructive modal used for the calculation of the peripheral and radial cracks in stretch z-flanges of Aluminum Alloy 5182 sheet (Butcher et al.,2006). Once more continuum mechanics-based method became utilized for the prophecy of peripheral and radical crack in Aluminum Alloy 5182 stretchable flange based on enlarge strain-based formation restraint curve (Simhaet al., 2008). Dewang et al. (2014) proclaimed the crack location in non-axisymmetric stretch flanges using finite element simulation by considering the effect of preliminary length of flange and punching die clearance. Die, punch and blank holder are used for stretchable flange forming operation during experiments (Wang et al., 1984; Dudra and Shah, 1988; Asnafi, 1999; Yeh et al., 2007; S. Kumar et al., 2000). Strain measurements are done experimentally using tool maker's microscope (Dudra and Shah, 1988; Wang et al., 1984) Radial and circumferential cracks are observed during stretch flanges using aluminum alloys (Chen et al., 2005; Butcher et al., 2006; Simha et al., 2008). Edge cracking and its location are also predicted experimentally using AA 5052 sheets. The present study aims to study the stretch flanging process using experimental methods and to simulate the stretching flange process using FEM software package ABAQUS (Dewang. Y, 2015). FEM simulations are done to investigate the influence of operational parametric characteristics such as preliminary length of flange, clearance of punching die, and width of sheet metal specimen on maximum thinning occurred in stretch flange forming.

MATERIALS BEHAVIOR

To evaluate the behavior of material under its mechanical deforming condition i.e., Aluminum Alloy 5052 sheets having thickness of 0.5-millimeter, tensile tests will be

performed. First, uniaxial tensile test samples are prepared as per American society of tool and manufacturing standard (ASTM E8/E8M-eleven) as shown in figure 3. After testing the samples, the behavior of the material is obtained in terms of the true stress-strain relationship as presented in figure.4. In table 1 properties of the material under external load condition as mentioned. For FEM analysis of the stretchable flanging operation, this stress-strain relationship along with properties (Mechanical) of Aluminum alloy 5052 sheets are employed.

Figure 3 Aluminum Alloy-5052 H-32^0 specimens for tension load testing.

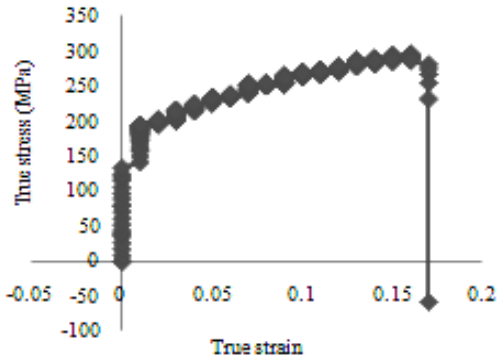

Figure 4 curves for absolute stress- strain for Aluminum Alloy-5052

Table 1 Properties of material AA 5052

Mechanical characteristics	Sheet of AA 5052
Density	2680 kg/m3
Elastic Modulus	70.3 GPa
Poisson's ratio	0.33

EXPERIMENTAL WORK

Stretch flanging tests are completed on a hydraulic press. After making stretch flanges of AA

5052 sheets, strain measurement is carried out with the help of a vernier caliper along the radial profile of die and the free fringe of the sheet. Initially, size and computations are done alongside radial profile of die as seen in figure 5. It is discovered by using manual dimension with the assist of vernier-caliper that

Initial width of sheet = 2.668 cm,

Width of arc along die profile radius = 2.45 cm,

Height of arc = 0.49 cm.

Mathematical calculations are done, and it is found that radius of arc =1.77625 cm, length of die arc = 87^0.

Now circumferential strain along die profile radii is obtained as

= (length of arc along die profile radii –initial width of sheet) / (initial width of sheet)

= (2.70350-2.668) / (2.668) = 1.33 %

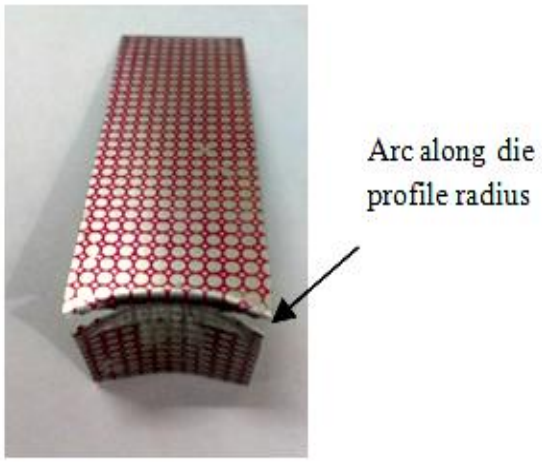

Figure 5 Stretch flange showing arc along die profile radius

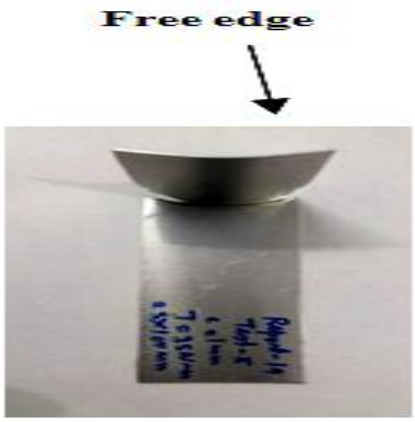

Figure 6 stretch flanges showing free edge

On the other hand, it is observed from figure 6. By manual measurement through vernier-caliper that

Initial width of sheet = 2.668 cm,

Width of arc along free edge = 2.66 cm,

Height of arc along free edge = 0.192 cm.

After these mathematical operations, it is found that radius of die arc = 4.70251 cm, length of arc along free edge = 2.69680 cm and angle subtended by die arc = 33^0 degree.

By using below formula, circumferential strain along free edge is calculated as

= (length of arc along free edge –initial width of sheet)/ (initial width of sheet)

= (2.70350-2.668)/ (2.668) = 1.33 %

FINITE ELEMENT ANALYSIS

Finite element method

In context of explicit dynamic FEM, the digitally work mathematical statement which involves inner force, forces applied on body, meeting force and momentum can be expressed as following :(Yeh et al., 2007)

$$\int \rho \ddot{x} \delta x \, dV + \int \sigma \delta \varepsilon \, dV - \int \rho b \delta x \, dV - \int f \delta x \, dS = 0 \int \rho \ddot{x} \delta x \, dV + \int \sigma \delta \varepsilon \, dV - \int \rho b \delta x \, dV - \int f \delta x \, dS = 0 \quad \ldots\ldots (1)$$

Wherein $\ddot{x}$ is for acceleration, σ used for Cauchy stress, ϵ is for change in dimension to original dimension, density is defined as ρ, b used as density of body force and f define traction force act on surface. After applying finite element discretion, Eq. (1) will be represented in a matrix formation as

$$M\ddot{u} = F_t^1 + F_t^2 + F_t^3 F_t^1 + F_t^2 + F_t^3 \quad \ldots\ldots\ldots (2)$$

and

$$M = \sum \int \rho N^T N dV$$

$$F_t^1 = \sum \int B^T \sigma \, dV$$

$$F_t^2 = \sum \int \rho N^T b \, dV$$

$$F_t^3 = \sum \int N^T f dS$$

Wherein M is used for mass matrix, $F_t^1 F_t^1$, $F_t^2 F_t^2$ and $F_t^3 F_t^3$ are the stress load, frame force load, and floor force load at time t, respectively. N denoted as shape feature. The solution for time t+ Δt can be acquired employing solving the acceleration in Equation (2) first off. Then, the relevant difference method was used to evaluated velocity and displacement as follows:

$$\ddot{u}_t = M^{-1}(F_t^1 + F_t^2 + F_t^3 \ddot{u}_t = M^{-1}(F_t^1 + F_t^2 + F_t^3) \quad \text{..... (3)}$$

$$v_{t+\frac{\Delta t}{2}} = v_{t-\frac{\Delta t}{2}} + \ddot{u}_t \Delta t_1 v_{t+\frac{\Delta t}{2}} = v_{t-\frac{\Delta t}{2}} + \ddot{u}_t \Delta t_1 \quad \text{..... (4)}$$

$$u_{t+\Delta t} = u_t + v_{t+\frac{\Delta t}{2}} \Delta t_{t+\frac{\Delta t}{2}} u_{t+\Delta t} = u_t + v_{t+\frac{\Delta t}{2}} \Delta t_{t+\frac{\Delta t}{2}} \quad \text{..... (5)}$$

Where

$$\Delta t_{\frac{t+\Delta t}{2}} = 0.5(\Delta t_t + \Delta t_{t+\Delta t}) \Delta t_{\frac{t+\Delta t}{2}} = 0.5(\Delta t_t + \Delta t_{t+\Delta t}),$$

V as velocity and u outline as displacement. Δt is the time increment inside the relevant distinction technique that must be small than an essential time increment Δtcri to ensure the convergence in the solution manner, and the crucial time increment Δtcri for the shell component within the explicit dynamic scheme is determined from Equation (6):

$$\Delta t_{cri} = \frac{L_S}{\sqrt{E/\rho(1-\theta^2)}} \Delta t_{cri} = \frac{L_S}{\sqrt{E/\rho(1-\theta^2)}} \quad \text{..... (6)}$$

Wherein Ls is the feature-length which became evaluated from the elementary region divides the longest aspect within the component. E used as elastic modulus and n for Poisson's ratio. Every component has its vital time increment, the important time increment in a deformation stage may be decided from the minimum value in the complete system.

i.e., Δtt+Δt= α min {Δt1, Δt2, . . ., Δtn} …… (7)

Wherein n is the component number. Δti is used as the important time increment for component i, and for safety, α is added as a safety parametrical agent which having presets cost to be 0.9 in the simulation. The time increasing in Eq. (6) is proportional to the square root of the mass density. Hence, the maximum merit of the specific dynamic is if the simulation results nevertheless maintain accuracy, it permits us to increase the velocity component or the mass density component to minimize the performing time under simulation.

FINITE ELEMENT SIMULATION

Finite element simulations of the stretchable flanging operation executed with the help of ABAQUS software which is one of the commercialized software and widely used for simulation work. The material properties of AA 5052 used for numerical simulation are

given in table 1. The isotropic hardening rule is considered for the material which behaves as elastic-plastic material. Figure 7 represent the finite element model used for stretch flanging process. Die has meshed with 3d shell-type feature which consists of R_3D_4 discrete rigid element type of 2734 elements and 2785 nodes using free meshing technique. The blank holder is discredited with a shell type feature which consists of 448 R_3D_4 discrete rigid elements and 492 nodes. Punch is meshed with4429 R_3D_4 quadrilateral discrete rigid elements and 4485 nodes.

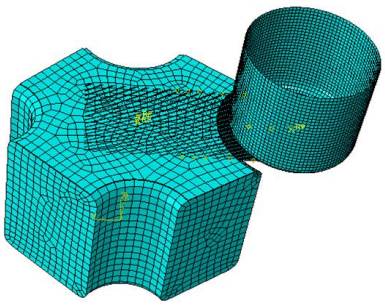

Figure 7 Finite element model of stretch flanging process

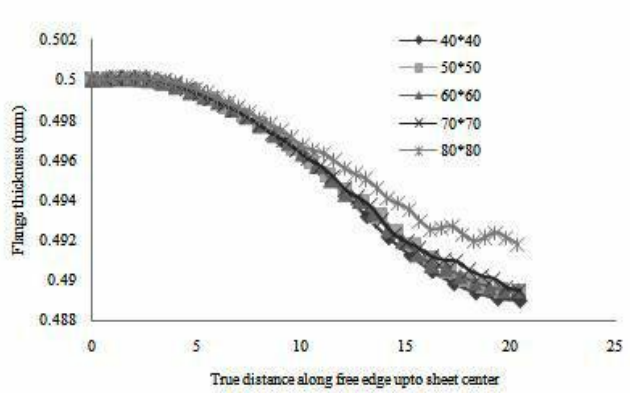

Figure 8 Flange thickness distributions along the free edge for mesh convergence of 40 mm width blank

The geometric and finite element model meshed consists of the following dimensions: Length of sheet metal blank = 100 mm, Width = 50 mm, blank thickness = 0.5 mm. The blank is considered as deformable and AA 5052. The blank is modeled using a four-node double curve thin shell component with reduced integration, S4R finite strain elements having 5 integration points through the thickness. It includes 7770 S4R quadrilateral discrete inflexible component and 7952 nodes. The clean holder is then authorized to alternate its position within the upward course to settled important modifications within the thickness. The coefficient of friction is 0.1 changed into described among one-of-a-kind contact surfaces. The die stays fixed in all instructions whilst the sheet becomes allowed as a loose

frame which is controllable through the contact boundary situation among the unique gear and sheet. The punching motion turned into described the use of a pilot node. This node is employed to gain the punch pressure to bend the sheet for the duration of a simulation. Punch was allowed to transport most effectively in a downward course while it was restrained in all different instructions. Finite element simulations have performed the usage of the radius of die and holder = 30 mm inside the gift examine.

MESH CONVERGENCE STUDY

In the present study to ascertain the validity of the finite element simulation results different types of meshes after partition are used and convergences of results are obtained. For the sheet metal blank of 40 mm width, it was found from figure 8. That flange thickness decreases along the free edge up to the sheet.

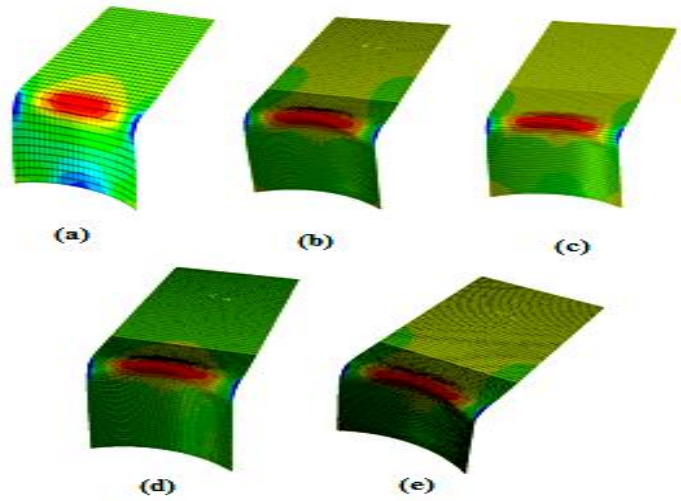

Figure 8 Contour plot of flange thickness for different meshes of 40 mm width blank (a) 40*40 (b) 50*50 (c) 60*60 (d) 70*70 (e) 80*80

Center is found to converge with the mesh size 60*60 as the flange thickness obtained at 60*60 and 70*70 are almost similar. With the repeatability of results obtained for two mesh sizes 60*60 and 70*70. Besides this, it is also observed that 60*60 mesh size gives accurate results with less computational time. Figure 9 shows the typical contour plots of the flange thickness of stretch flange at 100 % of punch travel for different mesh sizes. Hence in the present study 60*60 is the most appropriate size for a sheet metal blank of 40 mm.

RESULTS AND DISCUSSION

Influence of preliminary length of flange on Maximum Thinning (%)

In Figure 10 we observed the variation of maximum thinning (%) with the preliminary length of flange. It shows that maximizing thinning occurred in the flange increasing its non-linearly with an increment in preliminary flange length. One thing is very important to understand here that minimum flange thickness after the operation is obtained at the corner edges of the flange which can be clearly understood from the contour plot for flange thickness distribution. It is founded that an increment in preliminary length of flange from 20 mm to 40 mm, the maximum thinning (%) found to increase by 2 % approximately.

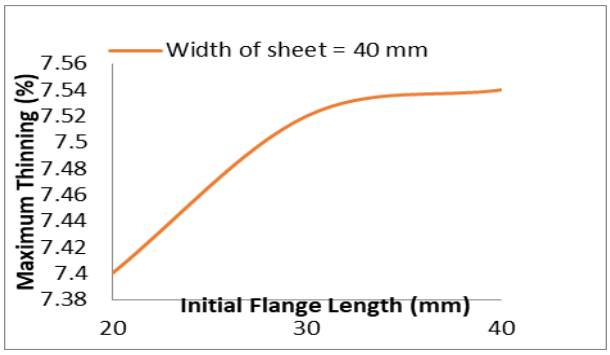

Figure 10 Effect of initial flange length on maximum thinning (%)

Influences of Punching die Clearance on Maximum Thinning (%)

Punch die clearance is the very prominent defining parameter that influences the stretch flange formability. Figure11 shows that the defining influences of punching die clearance on maximum thinning (%). It has been observed from the figure that when we increase punching die clearance its results in decreasing maximum thinning (%). The maximum thinning (%) is obtained at minimum clearance. It is very conclusive evidence to note that maximize thinning percentage reducing up to 3% with an increasing clearance of punching die from 0.5 millimeter to 1 millimeter.

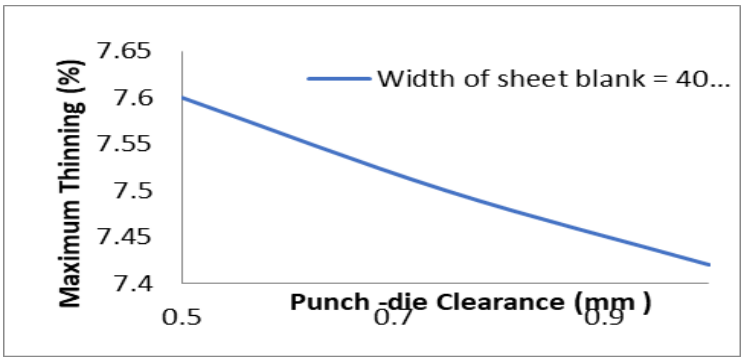

Figure 11 Effects on clearance of punching die with the max. Thinning (%) for width of 40 mm blank

Influence of a width of the sheet on Maximum Thinning (%)

The width of blank of sheet metal is another parameter of the stretch flanging process. By applying an unvarying blank holding force of 600 N, with three different widths of sheet metal blanks.i.e., 40 mm, 50 mm, and 60 mm. Figure 12 shows the influence of the width of sheet metal blank on maximum thinning (%) that occurred in stretch flange during operation. It is observed from the figure 12 that maximum thinning (%) increasing non-linearly as we increase width of the sheet metal blank. It is found that maximum thinning (%) increasing significantly by 38 % approximately with an increment in width of sheet used as specimen from 40 mm to 60 mm.

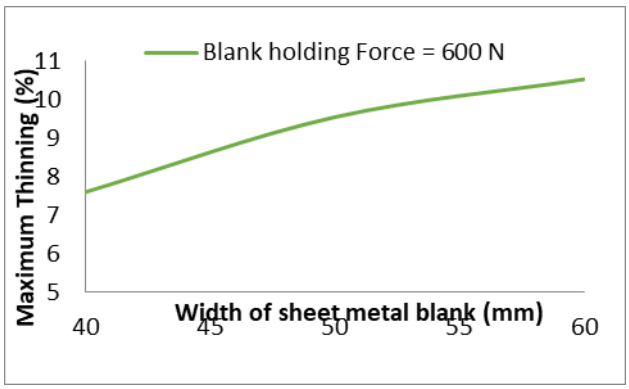

Figure 12 Influence of blank holding force on maximum thinning (%)

CONCLUSIONS

Experiments are conducted to evaluate strain that occurred in stretch flange along die profile radius and free edge. Besides this finite element simulations are also carried out using AA 5052 sheets. A Mesh modeling study was also executed to prove the results of the used FEM model to be accurate. It is found through experiments that very low strains are occurred both at the free edge and along die profile radii. It is found through finite element simulation that the width of sheet metal blank has a greater impact on maximum thinning percentage in the comparison to other process parametrical such as preliminary flange length and clearance in punch die. We also use an electro-hydraulic forming process for the enhancement of formability.

REFERENCES

Asnafi, N. 1999. On stretches and shrinks flanging of sheet aluminum by fluid forming. J. MatrProc Technol. 96,198-214.

Bao, Y.D., and Huh, H.2007. Optimum design of trimming line by one-step analysis for auto

body parts. J.of MatrProcTechnol. 187-188, 108–112.

Butcher, C., Chen, Z., andWorswick, W. 2006. A lower bound damage-based finite element simulation of stretch flange forming of Al-Mg alloys. Int. J. of Frac.142, 289-298.

Chen, Z., Worswick, M. J., Pilkey A. K. and Lloyd, D. J. 2005. Damage percolation during stretch flange forming of aluminum alloy sheet. J. MechPhy Solids. 53, 2692-2717.

Dudra, S., & Shah S. 1988. Stretch flanges: formability and trimline development. J. MatrShap. Technol. 6(2), 91-101.

Feng, X.,Zhongqin, L.,Shuhui, L., andWeili, X. 2004. Study on the influences of geometrical parameters on the formability of stretch curved flanging by numerical simulation. J. Matr Proc. Technol.145, 93-98.

Hu,P.,Li, D.Y. & Li, Y. X. 2003. Analytical models of stretch and shrink flanging. Int. J. Mach Tools &Manuf . 43, 1367–1373.

Li, D., Luo, Y., Peng, Y., & Hu, P. 2007. The numerical and analytical study on stretch flanging of V-shaped sheet metal.J. Matr. Proc. Technol. 189, 262–267.

Simha, C.H.M.,Grantab, R., &Worswick, M. J . 2008. Application of an extended stress-based forming limit curve to predict necking in stretch flange forming. J. ManufSci and Engg. 130, 1-11.

Wang, C. T., Kinzel, G., &Altan, T.1995. Failure and wrinkling criteria and mathematical modeling of shrink and stretch flanging operations in sheet–metal forming. J. Matr. Proc. Technol.53, 759-780.

Wang, N. M., Johnson, L.K., & Tang, S.C. 1984. Stretch flanging of "V"- shaped sheet metal blanks. J. Applied Metal Working.3, 281-291.

Worswick, M. J., and Finn, M.J. The numerical simulation of stretch flange forming. Int. J. Plasticity. 16,701-720.

Yeh, F. H., Wu, M. T., & Li, C.L. 2007. Accurate optimization of blank design in stretch flange based on a forward–inverse prediction scheme. Int. J. Mach Tools & Manuf.47, 1854–1863.

Dewang, Y., Hora, M.S., &Panthi, S.K.2014. Finite element analysis of non-ax symmetric stretch flanging process for prediction of location of failure. Procd. Matr. Sci. 5, 2054-2062.

Wang, N. M., Wenner, M.L.1974. An analytical and experimental study of stretch flanging. Int. J .Mech. Sci. 16,135-143.

Wang, N.M. An analytical and experimental study of notched stretch flanges. 1983. AIME, 309-318.

Wang C.T. et al.1974. Wrinkling criterion for an anisotropic sheet with compound curvatures in sheet forming. Int.J. Mech. Sci. 36, 945-960.

S.Kumar et al. 2020. Effect of punch profile on deformation behavior of AA5052 sheet in stretch flanging process. Archives of civil and mechanical engg. 20, 18-28.

Dewang Y. et al. 2015. Prediction of crack location and propagation in stretch flanging process of aluminum alloy AA-5052 sheet using FEM simulation. Trans Nonferrous Metals Soc China. 2015; 25(7); 2308.